

- (10) Bates, F. S.; Cohen, R. E. *Macromolecules* 1981, 14, 881.
- (11) Ramos, A. R.; Cohen, R. E. *Polym. Eng. Sci.* 1977, 17, 639.
- (12) Kato, K. *J. Polym. Sci., Polym. Lett. Ed.* 1966, 4, 35.
- (13) Hosemann, R.; Bagchi, S. N. "Direct Analysis of Matter by Diffraction"; North-Holland Publishing Co.: Amsterdam, 1962.
- (14) Cohen, J. B. "Diffraction Methods in Materials Science"; Macmillan: New York, 1966.
- (15) Guinier, A.; Fournet, G. "Small-Angle Scattering of X-Rays"; Wiley: New York, 1955.
- (16) Koberstein, J. T.; Morra, B.; Stein, R. S. *J. Appl. Crystallogr.* 1980, 13, 34.
- (17) Stribeck, N. Ph.D. Dissertation, Philipps-Universität, Marburg/Lahn, 1980.
- (18) Brandrup, J.; Immergut, E. H., Eds. "Polymer Handbook", 2nd ed.; Wiley: New York, 1975.

Electrohydrodynamic Instabilities in the Nematic Phase of a Homopolyester from 4,4'-Dihydroxy- α -methylstilbene

William R. Krigbaum,* Clara E. Grantham, and Hiro Toriumi

Department of Chemistry, Gross Chemical Laboratory, Duke University, Durham, North Carolina 27706. Received August 13, 1981

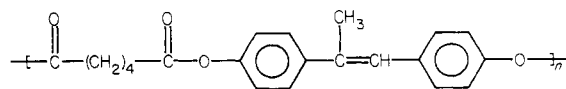
ABSTRACT: Electric field induced flow instabilities are examined for a nematogenic homopolyester of low molecular weight, P-6, synthesized from 4,4'-dihydroxy- α -methylstilbene and adipic acid. The observations for P-6 are compared with the behavior of the low molecular weight nematogen (*p*-methoxybenzylidene)-*p*-*n*-butylaniline (MBBA) and with those reported previously for a high molecular weight nematogenic copolyester, T2/60. In the conduction regime, P-6 forms a fluctuating Williams domain pattern in a few tenths of a second, while some hours are required to form a Williams domain pattern in T2/60. P-6 also differs from T2/60 in exhibiting a dynamic scattering mode. At threshold this pattern has a formation time of several seconds, which allows examination of its precursor pattern.

Introduction

Thermotropic nematic phases have been reported for a variety of polymers containing mesomorphic groups on the side chain or incorporated in the main chain. Recently, there has been increased interest in polymers having main-chain mesomorphism due to their potential application for the production of high-modulus fibers. These polymers may exhibit nematic, smectic, cholesteric, or twisted smectic mesophases or some combination of these in different temperature ranges. Identification of the type of mesophase is thus an important step in the characterization of these materials. Two of the more definitive procedures for characterization of low molecular weight mesogens, X-ray diffraction and mutual miscibility, have thus far not been widely applied to the characterization of polymeric mesophases. The presence of a nematic phase in a low molecular weight mesogen is often evidenced by the appearance, when viewed under the polarizing microscope, of "threads" in a birefringent fluid phase. Alternatively, the differential scanning calorimeter (DSC) can be used to distinguish between thermotropic nematic and smectic phases by the magnitude of the enthalpy change accompanying the transition to the isotropic phase. The interpretation of these same types of observation for polymeric mesophases is often less certain. A remnant of high-melting crystallites may produce what appears to be an anisotropic fluid phase,¹ and on occasion the threadlike pattern of disclinations forms with great reluctance (or not at all) in a highly viscous polymeric nematic phase. Also, the interpretation of DSC data for polymeric mesophases may be complicated by transitions involving different crystalline polymorphs and by a variable degree of supercooling, which appears to be characteristic of the isotropic-nematic transition in polymers. Further, the paucity of experimental data precludes a confident prediction of the magnitude of the enthalpy changes expected for transitions of the different types of mesophases in

polymers. These difficulties led to the exploration^{2,3} of electric field induced instabilities as a possible confirmatory test for the presence of a thermotropic nematic phase in polymers. The first investigations were performed with Tennessee Eastman T2/60, a poly(ethylene terephthalate-co-1,4-benzoate) containing 60 mol % *p*-oxybenzoyl units. Electrohydrodynamic instabilities observed in this polymeric nematic phase included the analogues of the Williams domain pattern,⁴ the variable grating mode,^{5,6} and high-field turbulence.⁷ These observations were compared^{2,3} with the corresponding instability patterns seen in *p*-azoxyanisole (PAA), the classical low molecular weight thermotropic nematogen. Analogues of the chevron pattern⁸ and the dynamic scattering mode (DSM)⁹ were not observed in this polymer.

These results gave promise that electric field effects might furnish a useful diagnostic tool for nematic phases in polymers. On the other hand, it was recognized² that additional work on a variety of polymers would be required to assess the generality of this procedure as a confirmatory test. In the present paper we report the results of a study of electric field effects using a polyester synthesized from 4,4'-dihydroxy- α -methylstilbene and adipic acid.^{10,11}



One of the disadvantages of the use of electrohydrodynamic effects for diagnostic purposes, as revealed by our earlier studies, is the long formation time on the instability patterns. For example, the formation time of Williams domain patterns in T2/60 was of the order of an hour, as compared to tenths to hundredths of a second in PAA. We presumed this difference was due to the high viscosity of the polymeric mesophase. If this explanation is correct, it should be possible to reduce the formation time by examining polymeric samples of low molecular weight. The

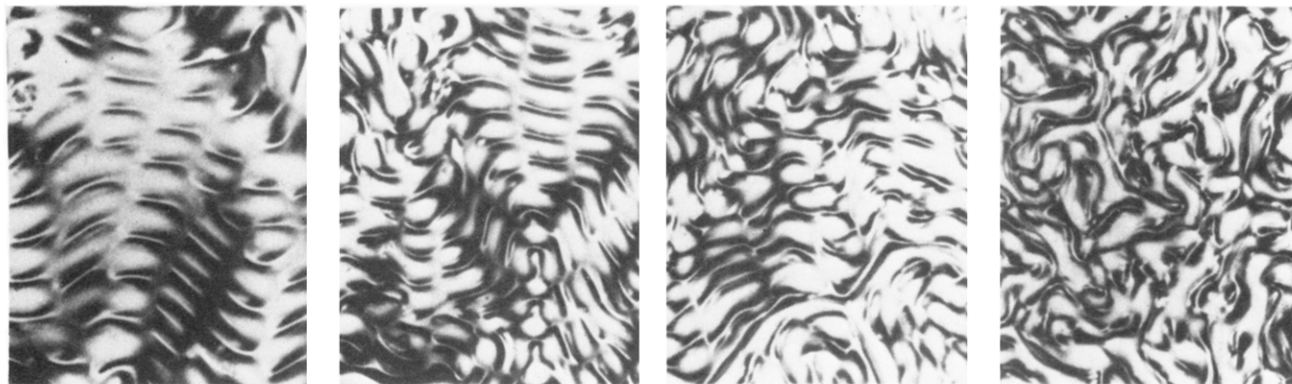


Figure 1. FWD pattern observed for a 20- μm -thick sample of polymeric P-6 at 195 $^{\circ}\text{C}$ at a frequency of 30 Hz. Voltages for micrographs a–d are 7, 8, 9, and 10 V, respectively.

behavior of an oligomeric sample will be investigated here to test this hypothesis.

Experimental Section

The sample of the polyester, designated P-6, was synthesized by the method previously described.¹¹ Its inherent viscosity, as measured at 25 $^{\circ}\text{C}$ in a 60:40 mixture of phenol and tetrachloroethane, was 0.15 dL/g. The sample of (*p*-methoxybenzylidene)-*p*-*n*-butylaniline (MBBA) was obtained from Aldrich Chemical Co. and was used without further purification.

The liquid crystalline samples were placed between two slides having a transparent conductive coating of tin oxide, and the temperature was controlled by a Mettler FP52 hot stage. The Chatelain rubbing technique¹² was used in an attempt to obtain samples having an aligned, planar texture, and the sample thickness was controlled by mica spacers. The ac voltage source was a Wavetek Model 110 generator followed by a linear audio amplifier. The samples were viewed with a Bausch and Lomb microscope with a crossed polarizer and analyzer, and photomicrographs at an original magnification of 75 \times were taken with a Nikon PMF photoattachment.

Results and Discussion

The P-6 sample melted to form a nematic phase at 164 $^{\circ}\text{C}$, and a biphasic region extended from 216 to above 300 $^{\circ}\text{C}$, where decomposition occurred. Electrohydrodynamic effects were examined in the temperature range of the nematic phase, 175–210 $^{\circ}\text{C}$.

As previously observed for T2/60, the rubbing technique failed to produce a nematic sample of P-6 having a uniform, uniaxial alignment of the molecules. The pattern observed at 195 $^{\circ}\text{C}$ in a 20- μm sample at the threshold voltage of 7 V and 30 Hz is shown in Figure 1a. An irregular pattern of diffuse light lines was formed immediately upon application of this voltage, and the pattern appearing in Figure 1a developed in a few tenths of a second. This observation confirms our postulate that the domain formation time in polymers is principally governed by the viscosity of the nematic phase and that short formation times can be achieved by keeping the molecular weight of the polymer low. Micrographs 1a–d illustrate the progressive changes in the instability pattern as the voltage was raised from 7 to 10 V in 1-V increments, keeping the frequency and temperature fixed.

Regions of different orientation are evident in Figure 1a, and the boundaries of these regions tended to develop along the nematic “threads” that were visible before application of the electric field. Although failure to achieve a uniformly aligned sample complicates the interpretation, it is immediately evident that this flow pattern differs significantly from that previously seen under corresponding conditions in T2/60. In the latter case the characteristic feature consisted of a bright line bordered by two dark lines, and this feature resembled the Williams domain

pattern formed in an unoriented sample of the low molecular weight nematogen, PAA. For an aligned, planar sample of PAA the Williams domain pattern consists of parallel bright lines extending perpendicular to the rubbing direction and having a periodicity approximately equal to the sample thickness. This pattern was explained by Penz^{13,14} as arising from a vortex motion of the fluid in parallel cylinders, which act as a set of cylindrical lenses to focus light into parallel lines.

The pattern in Figure 1a has short sections consisting of a bright line bounded by two dark lines (appearing horizontally in the photograph) which resemble Williams domains. However, these are interrupted at regular intervals, giving a two-dimensional periodicity, which is quite foreign to the Williams domain pattern. In discussing this difference, we will refer to the usual coordinate system having x along the rubbing direction and z along the field direction. The cylindrical flow domains of the Williams pattern lie along the y direction, as mentioned above, and investigation with light polarized along the x or y directions indicates that the molecules are aligned in the xz plane.¹⁵ Theoretical treatments^{8,16–18} of flow instabilities induced by electric fields involve only these two dimensions. The predicted effects are a conduction regime below a critical frequency, f_c , having a threshold voltage, and a dielectric regime above f_c which appears at a critical value of the electric field. The characteristic features of the Williams domain (WD) pattern, which has one-dimensional periodicity, agree quite well with the predictions for the conduction regime. In particular, it has a threshold voltage, while the chevron pattern in the dielectric regime is electric field dependent, in agreement with theory. On the other hand, it seems evident to us that such two-dimensional theories cannot predict an instability having periodicity along two directions. The DSM, which appears in the conduction regime at higher voltages, is also not accounted for by theory.

As early as 1971 Aslaksen and Ineichen¹⁹ showed by laser diffraction that for voltages between the threshold voltage for the WD, V_t , and the onset of the DSM, the Williams domain pattern changes to one having two-dimensional periodicity. A more extensive study of this pattern in MBBA by Quon and Wiener-Avnear,²⁰ using laser diffraction and light microscopy, led them to ascribe the two-dimensional periodicity to a regular twisting of the Williams domains in which one domain rejoined its second neighbor. This pattern is now referred to as the fluctuating Williams domain (FWD). It had appeared in a photograph of MBBA under dc excitation by Durand, Veyssié, Rondelez, and Léger¹⁶ in 1970, although these authors did not comment upon this particular aspect of the pattern. Review of the literature indicates that various types of pat-

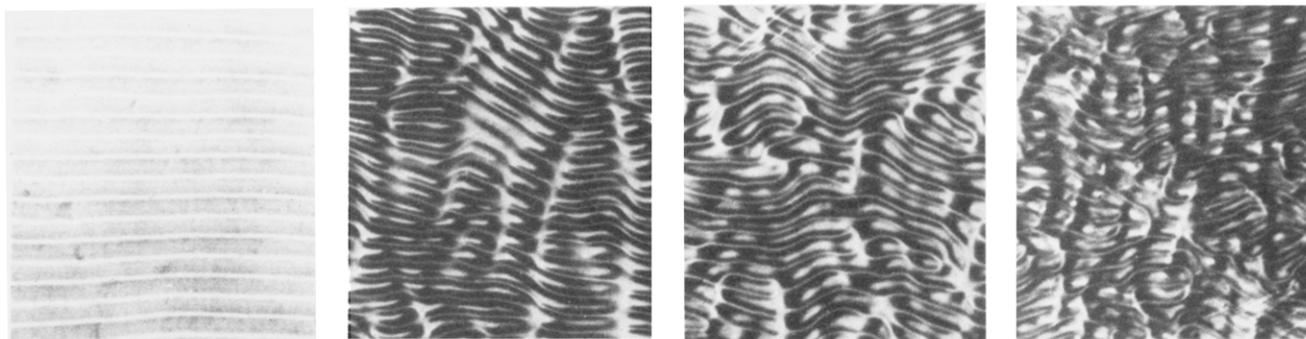


Figure 2. FWD pattern exhibited by a 20- μm sample of low molecular weight MBBA at 20 $^{\circ}\text{C}$. The frequency is 5 Hz and the voltages for micrographs a–d are 5.5, 7, 8, and 10 V, respectively.

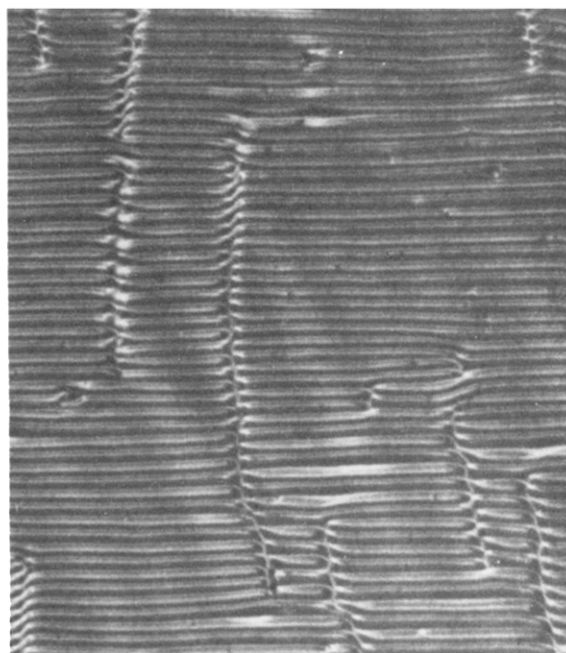


Figure 3. MBBA domain pattern at 20 $^{\circ}\text{C}$ in a 90 $^{\circ}$ twist cell of thickness 16 μm at 10 V and 100 Hz.

terns having two-dimensional periodicity have been reported for different low molecular weight nematogens under a variety of experimental conditions.^{21–31} Examination of these observations led us to conclude that the instability pattern shown for polymeric P-6 in Figure 1a most closely resembles the FWD pattern seen in MBBA. A detailed study of electric field effects observed in MBBA has been made by Bolomey and Dimitropoulos²⁸ and Hirakawa and Kai,³⁰ and we will summarize their findings.

The normal Williams domain pattern appears under ac excitation at a threshold voltage, V_t . At a slightly higher voltage the domains develop long-wavelength undulations of small amplitude, as illustrated for MBBA in Figure 2a. This is more clearly seen in Figure 1 of ref 28. As the voltage is further increased these undulations increase in amplitude and, at a voltage V^* , the periodic switching motion described above sets in. This marks the onset of the FWD. The pattern has two-dimensional periodicity because the twists are regularly spaced along a domain, and the twists in a group of adjacent domains tend to lie along a line parallel to the x direction, as shown in Figure 2b. The same photograph also illustrates the oscillation of the remaining segments of Williams domains out of the y direction. Nasta et al.³¹ pointed out that a possible precursor to the FWD pattern can be observed for MBBA in twist cells. As illustrated in Figure 3, this consists of irregular columns of discontinuities in the WD pattern. At

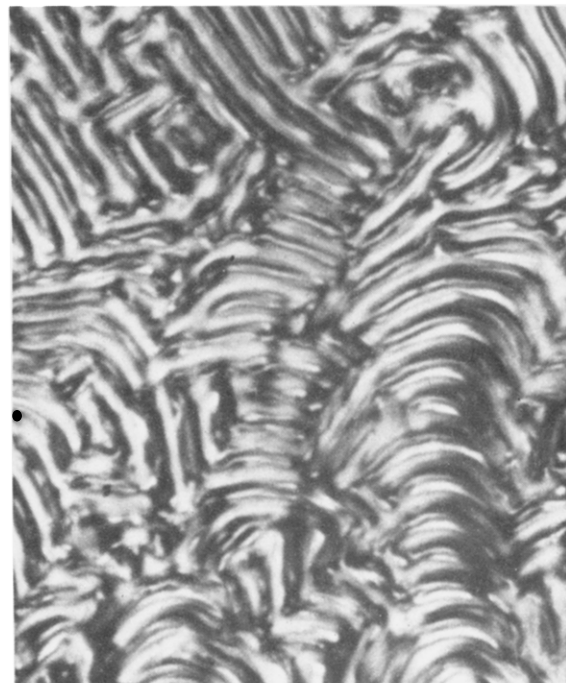


Figure 4. Pre-DSM pattern observed in a 10- μm sample of polymeric P-6 at 195 $^{\circ}\text{C}$ under 20 V at 30 Hz.

this stage the discontinuities are not yet regularly spaced along the Williams vortices, so there is only one-dimensional periodicity. Returning to the FWD pattern, we see that with further increase in voltage the crossovers become more numerous and the tilt out of the y direction increases, as seen in Figure 2c. In the last photograph in this series the regular periodicity is lost along both directions. A similar progression of the pattern with increasing voltage is found for P-6 in Figure 1a–d. The similarity of Figure 1b for P-6 with Figure 2b for MBBA is rather striking if one takes into account the failure of the rubbing technique to produce a uniformly aligned sample of P-6.

For MBBA the rather disordered pattern of Figure 2d changes, after a period of time, to a regular bidimensional grid pattern (GP), and at still higher voltages this gives way to the DSM. In polymeric P-6 we have not been able to observe the GP, but a higher voltage does produce the DSM. Upon application of 20 V, which is sufficient to form the DSM, the latter does not appear instantaneously but is preceded by the pattern shown in Figure 4. This is difficult to characterize due to the existence of regions differing in orientation in the original sample. It is more regular than the pattern at lower voltage shown in Figure 1d and may be broken Williams domains. After several seconds this is replaced by the DSM shown in Figure 5. This is not as spectacular as the corresponding pattern seen

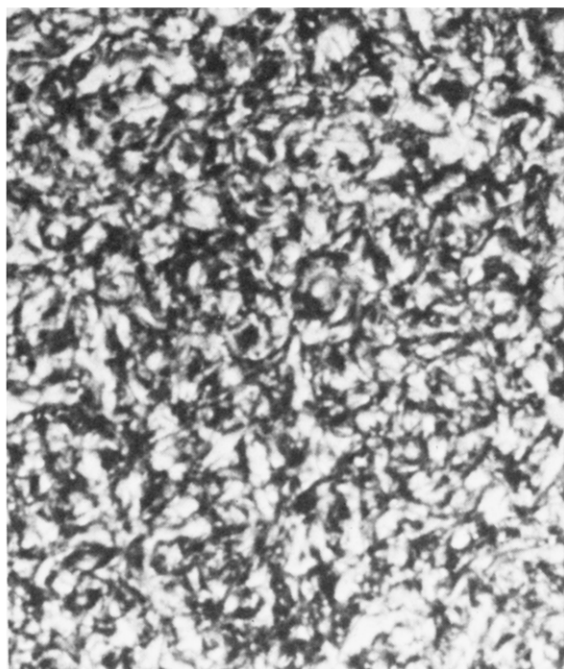


Figure 5. DSM pattern observed in P-6 under the conditions of Figure 4, but a few seconds later.

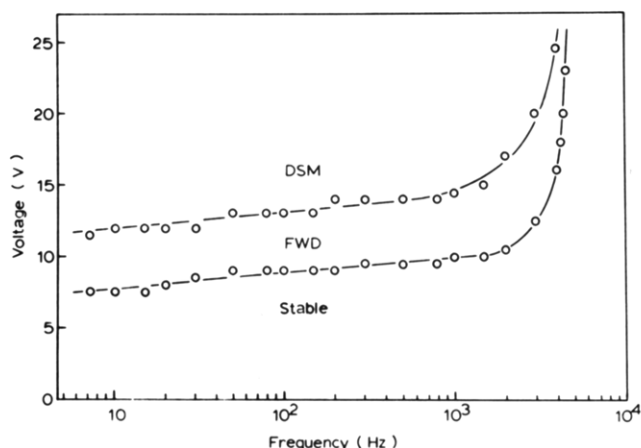


Figure 6. Frequency dependence of the threshold voltage for FWD and DSM in a 20-μm sample of P-6 at 190 °C.

in low molecular weight nematics, but it should be recalled that no DSM was found for the higher molecular weight copolymer, T2/60.

Unlike Williams domains, which are stable over a wide range of conditions, the range of stability of the FWD and GP is more restricted. Both the latter show a dependence upon the voltage, frequency, temperature, and sample thickness. Figure 6 illustrates the voltage–frequency curve for a P-6 sample of thickness 20 μm at 190 °C. The ac threshold voltage, V^* , increases slowly with frequency past 1 kHz and then diverges at a critical frequency of approximately 5 kHz. The shape of this curve is in qualitative agreement with that predicted for the threshold voltage of the WD pattern by the relation of Dubois-Violette, de Gennes, and Parodi:¹⁸

$$V_t = V_H \{ (1 + 4\pi^2 \tau^2 f^2) / (1 - f^2/f_c^2) \}^{1/2} \quad (1)$$

Here V_H is the Helfrich dc threshold voltage and τ is the dielectric relaxation time. The ratio of the threshold voltages of the DSM and FWD patterns in P-6 is approximately 1.5. Comparison with the results of Hirakawa and Kai³⁰ for high- and low-purity MBBA samples indi-

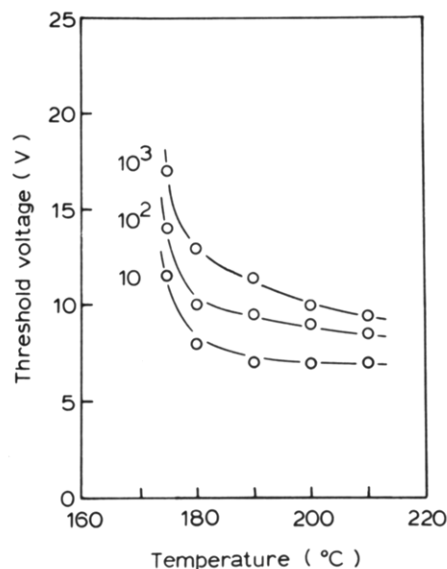


Figure 7. Temperature dependence of the threshold voltage for FWD in a 28-μm sample of P-6 at frequencies of 10, 100, and 1000 Hz.

cates this ratio for P-6 is relatively low, probably due to impurities which increase the conductivity. The f_c value of 5 kHz for P-6 is high relative to values measured for pure MBBA samples, again indicating the presence of impurities. The Orsay Liquid Crystal Group⁸ has reported that f_c of MBBA can be increased from 50 Hz to 3 kHz by doping with ionizable molecules. The dependence of the critical frequency upon conductivity can be seen from the relation

$$f_c = (\zeta^2 - 1)^{1/2} / 2 \quad (2)$$

where ζ is the Helfrich parameter and τ is the dielectric relaxation time, given by

$$\tau = \epsilon_{||} / 4\pi\sigma_{||} \quad (3)$$

Here $\epsilon_{||}$ and $\sigma_{||}$ are the dielectric constant and conductivity, respectively, both measured along the major axis of the nematogenic molecule. Equations 2 and 3 predict that dopants that increase the conductivity of the nematic phase will decrease the dielectric relaxation time, τ , and increase the critical frequency.

The temperature dependence of the threshold voltage for the FWD, as measured for a 28-μm-thick sample of P-6 at three frequencies, is illustrated in Figure 7. If the frequency is fixed, then V^* is seen to decrease with increasing temperature, T . Data (not shown) similar to those appearing in Figure 6, but for other temperatures, indicate that f_c increases with T . These two trends are in agreement with the more extensive observations of Gosciński and Léger²⁵ and of Dvorjetski et al.³² The former workers discussed the origin of the variation of V^* with T ; however, a decrease of V^* with T can be predicted in a qualitative sense from eq 1 due to the increase of f_c with T .

The variation of V^* with temperature for a fixed frequency of 1 kHz is shown for three sample thicknesses in Figure 8. One sees that for a fixed temperature, V^* increases as the sample thickness is increased. As indicated above, the threshold voltage, V_t , for the onset of Williams domains is independent of sample thickness. Hirakawa and Kai³⁰ report, in agreement with our observations for P-6, that V^* for MBBA increases with increasing sample thickness. There appears to be no data concerning the dependence of the threshold voltage of the grid pattern in MBBA with sample thickness. However, Bolomey and Dimitropoulos²⁸ give ranges of voltage within which the

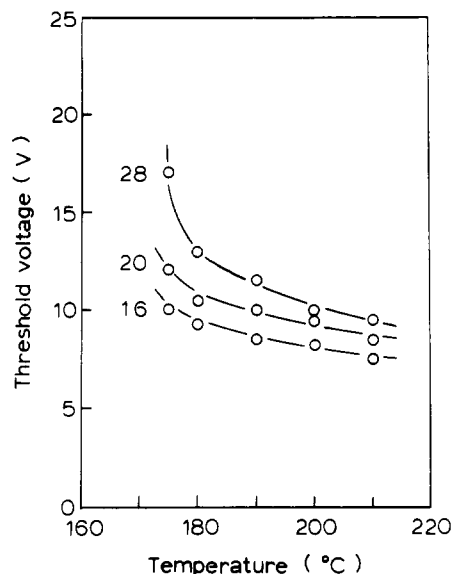


Figure 8. Temperature dependence of the threshold voltage for FWD in P-6 at 1000 Hz. Curves are shown for three sample thicknesses.

GP was observed for two sample thicknesses. These data suggest that the threshold voltage for the GP decreases with increasing sample thickness. Thus the WD, FWD, and GP differ in the widths of their respective ranges of stability and in the dependence of the respective threshold voltages on sample thickness.

Conclusions

The behavior of T2/60 in an electric field was found to be analogous to that of low molecular weight PAA, while MBBA appears to be a more appropriate model substance for P-6. Theory offers no explanation for the different behavior of MBBA and PAA in the conduction regime. One known difference between these two nematogens involves flexoelectricity or piezoelectricity, a concept first introduced by Meyer.³³ Schmidt, Schadt, and Helfrich³⁴ demonstrated that MBBA has a measurable flexoelectric coefficient, while the same does not appear to be true of PAA. However, any possible effect of flexoelectricity upon electrohydrodynamic instability patterns has not been treated theoretically.

A second objective of this work is to extend the observations reported previously for T2/60 to aid in assessing the generality of those results. Both polymers exhibit a type of instability pattern (WD or FWD) in the conduction regime which indicates that both have negative dielectric anisotropy and positive conductivity anisotropy. We have shown that the time required to form electrohydrodynamic instability patterns in polymeric nematic phases can be reduced considerably by working with polymers of low molecular weight. This will not generally require additional effort since a laboratory synthesizing a novel nematogenic polymer will usually prepare samples covering a range of molecular weights. On the other hand, the threadlike pattern characteristic of the nematic phase may also form more readily if the viscosity is reduced.

We believe electrohydrodynamic instabilities of polymers deserve further study, due both to their potential use for identification purposes and to the possibility that novel

observations will result when some of the parameters are extended into new ranges not accessible with low molecular weight mesogens. Only the low molecular weight sample of P-6 exhibited the DSM. This pattern appeared at the threshold voltage only after a delay of several seconds, which may be of interest since it allows time to photograph the pattern of the precursor. In the case of P-6, this precursor is much more regular than the flow pattern that appears at somewhat lower voltages. So far as we are aware, it has not been possible to photograph the pattern of any precursor to the DSM for low molecular weight nematogens.

Acknowledgment. We express our appreciation to the U.S. Army Office for support of this work (Grant DAAG 29-81-K-0023).

References and Notes

- Lader, H. J.; Krigbaum, W. R. *J. Polym. Sci., Polym. Phys. Ed.* **1979**, *17*, 1661.
- Krigbaum, W. R.; Lader, H. J.; Ciferri, A. *Macromolecules* **1980**, *13*, 554.
- Krigbaum, W. R.; Lader, H. J. *Mol. Cryst. Liq. Cryst.* **1980**, *62*, 87.
- Williams, R. J. *Chem. Phys.* **1963**, *39*, 384.
- Vistin', L. K. *Sov. Phys.—Crystallogr. (Engl. Transl.)* **1970**, *15*, 514, 908.
- Greubel, W.; Wolff, V. *Appl. Phys. Lett.* **1971**, *19*, 213.
- Gruler, H.; Meier, G. "Liquid Crystals, 3"; Brown, G. H., Labes, M. M., Eds.; Gordon and Breach: New York, 1972; Part II, p 779.
- Orsay Liquid Crystal Group. *Mol. Cryst. Liq. Cryst.* **1971**, *12*, 251.
- Heilmeyer, G.; Zanoni, L.; Barton, L. *Proc. IEEE* **1968**, *56*, 1162.
- Roviello, A.; Sirigu, A. *Gazz. Chim. Ital.* **1977**, *107*, 333.
- Krigbaum, W. R.; Ciferri, A.; Preston, J.; Asrar, J.; Toriumi, H. *Mol. Cryst. Liq. Cryst.* **1981**, *76*, 79.
- Chatelain, P. *Acta Crystallogr.* **1948**, *1*, 315.
- Penz, P. A. *Phys. Rev. Lett.* **1970**, *24*, 1405. *Ibid.* **1970**, *25*, 489.
- Penz, P. A. *Mol. Cryst. Liq. Cryst.* **1971**, *15*, 141.
- Carr, E. F. *Mol. Cryst.* **1969**, *7*, 253.
- Durand, G.; Veyssié, M.; Rondelez, F.; Léger, L. C. R. *Hebd. Seances Acad. Sci., Ser. B* **1970**, *270*, 97.
- Helfrich, H. W. *J. Chem. Phys.* **1969**, *51*, 4092. *Ibid.* **1970**, *52*, 4318.
- Dubois-Violette, E.; de Gennes, P. G.; Parodi, O. *J. Phys. (Paris)* **1971**, *32*, 305.
- Aslaksen, E. W.; Ineichen, B. *J. Appl. Phys.* **1971**, *42*, 882.
- Quon, W. S.; Wiener-Avnear, E. *Solid State Commun.* **1974**, *15*, 1761.
- Assouline, G.; Dmitrieff, A.; Hareng, M.; Leiba, E. *J. Appl. Phys.* **1971**, *42*, 2567.
- Kapustin, A. P.; Trofimov, A. N.; Chuvyrev, A. N. *Sov. Phys.—Crystallogr. (Engl. Transl.)* **1972**, *17*, 157.
- Wright, J. J.; Dawson, J. F. *Phys. Lett. A* **1973**, *43A*, 145.
- Kai, S.; Yamaguchi, K.; Hirakawa, K. *Jpn. J. Appl. Phys.* **1975**, *14*, 1653.
- Goscianski, M.; Léger, L. *J. Phys. Colloq. (Paris)* **1975**, *C1*, 231.
- Berman, A. L.; Gelerinter, E.; de Vries, A. *Mol. Cryst. Liq. Cryst.* **1976**, *33*, 55.
- Pikin, S.; Ryschenkov, G.; Urbach, W. *J. Phys. (Paris)* **1976**, *37*, 241.
- Bolomey, P. H.; Dimitropoulos, C. *Mol. Cryst. Liq. Cryst.* **1976**, *36*, 75.
- Weir, R. C.; Gelerinter, E. *Mol. Cryst. Liq. Cryst.* **1977**, *40*, 199.
- Hirakawa, K.; Kai, S. *Mol. Cryst. Liq. Cryst.* **1977**, *40*, 261.
- Nasta, L.; Lupu, A.; Beica, T.; Serban, T.; Matei, L.; Giurgea, M. *Mol. Cryst. Liq. Cryst.* **1979**, *53*, 137.
- Dvorjetski, D.; Silberberg, Y.; Wiener-Avnear, E. *Mol. Cryst. Liq. Cryst.* **1977**, *42*, 273.
- Meyer, R. B. *Phys. Rev. Lett.* **1969**, *22*, 918.
- Schmidt, D.; Schadt, M.; Helfrich, W. *Z. Naturforsch.* **1972**, *27*, 277.